E7.4-10.45.2.
CR-137441

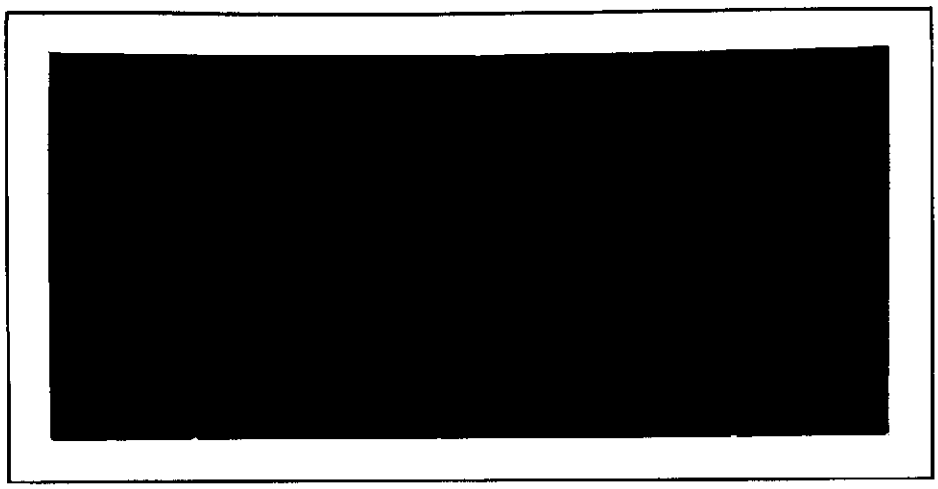

SCIENCE APPLICATIONS INCORPORATED

N74-21977

(E74-10452) DETERMINATION OF AEROSOL CONTENT IN THE ATMOSPHERE FROM ERTS-1 DATA Final Report, 7 Sep. 1972 - 6 Oct. 1973 (Science Applications, Inc.) 55 p HC $5.75 CSCL 04A

G3/13 00452

Unclas

DETERMINATION OF AEROSOL CONTENT IN THE ATMOSPHERE FROM ERTS-1 DATA

M. Griggs

Final Report

Contract No.: NAS5-21860

Proposal Number: 245

GSFC ID Number: P 135

SCIENCE APPLICATIONS, INC.
1200 Prospect Street
P. O. Box 2351
La Jolla, California 92037

Prepared for:

GODDARD SPACE FLIGHT CENTER

23 October 1973

TABLE OF CONTENTS

LIST OF FIGURES

FOREWORD

This report documents the research performed under contract NAS5-21860 between 7 September 1972 and 6 October 1973. Dr. M. Griggs was the Principal Investigator, and Dr. C. B. Ludwig and Dr. W. Malkmus were co-investigators.

The author is indebted to Dr. R. S. Fraser, the contract monitor, for many stimulating discussions, and to Mr. G. Hall for making some of the ground-truth measurements at the Salton Sea.

DETERMINATION OF AEROSOL CONTENT IN THE ATMOSPHERE FROM ERTS-1 DATA

M. Griggs
Science Applications, Inc.

SUMMARY

Significant results, relating the radiance over water surfaces to the atmospheric aerosol content, have been obtained. The results indicate that the MSS channels 4, 5 and 6 centered at 0.55, 0.65 and 0.75 μm have comparable sensitivity, and that the aerosol content can be determined within ± 10% with the assumed measurement errors of the MSS. The fourth channel, MSS 7, is not useful for aerosol determination due to the water radiance values for this channel generally being less than the instrument noise. The accuracy of the aerosol content measurement could be increased by using an instrument specifically designed for this purpose.

This radiance-aerosol content relationship can possibly provide a basis for monitoring the atmospheric aerosol content on a global basis, allowing a base-line value of the global burden of aerosols to be established. This base-line could probably be established more rapidly from satellite measurements than from a network of ground-based observations. In addition, this technique could possibly provide a method for monitoring the particulate emissions of the SST's, by making observations in the vicinity of flight corridors, such as over the North Atlantic. It may be possible to look at the ocean through the flight corridor and alongside it and measure the difference due to the SST's in the aerosol content.

Further studies of the radiance-aerosol content relationship are needed to establish the global applicability of the results, and to confirm that the effects of sun glitter are minimal as indicated in this program. These studies could utilize future ERTS-1 and ERTS-B data at the existing test sites. Cooperation with other agencies such as EPA and NOAA, who make Volz observations, would allow the studies to be expanded to national and global scales. ERTS-1 data obtained over the USA since August 1972 should also be analyzed in conjunction with aerosol data from the turbidity network of Volz photometers operated by EPA.

The contrast-aerosol content investigation show useful linear relationships in MSS channels 4 and 5, allowing the aerosol content to be determined within $\pm$ 10%. MSS 7 is not useful due to the low accuracy in the water radiance, and MSS 6 is found to be too insensitive. These results rely on several assumptions due to the lack of ground-truth data, but do serve to indicate which channels are most useful.

1. INTRODUCTION

The scientific community (e.g. SCEP[1] and SMIC[2]) has become increasingly aware in recent years of the importance of atmospheric aerosols and their optical properties in possible climate modification. The aerosols in the atmosphere consist of man-made and natural particles, and it is the man-made contribution due to combustion added to the natural (dust, sea spray, forest fires and volcanic dust) background that is generally considered to be important in determining climatic changes. However, the man-made contribution on a global scale is quite small; estimates range from a negligible amount[3] to about 6% of the natural background[4]. (Of course, on a local scale, e.g. the Los Angeles basin, man-made particles can far exceed the natural concentration.) It may well be that global changes in the natural background are more important than man-made particles. With the increased cultivation of land and activities of man in arid areas, the background level of aerosols is likely to increase.

McCormick and Ludwig[5] presented evidence of a worldwide buildup of atmospheric aerosols which could increase the earth albedo resulting in a cooling of the earth-atmosphere system. This effect would counteract the postulated increase of temperature in the lower atmosphere due to the "greenhouse effect" of the increased CO_2 emissions by human activities. In fact, there has been a decrease in the mean annual air temperature since about 1945 at mid latitudes, suggesting that the aerosol pollution effect is greater than that of the CO_2 increase. However, the effects of aerosols and CO_2 are more complex than suggested above, so that their effects on climate are not readily predicted. For instance, Robinson[6] points out that the earth may self-regulate its temperature by the variation of cloud amount: the higher temperatures, due to the CO_2 "greenhouse effect", lead to a higher water content in the lower atmosphere, which may increase the

cloud amount; this increases the albedo, thereby decreasing the temperature. Robinson concludes there is no justification for forecasting a final equilibrium temperature due to an increase in CO_2 content, until atmospheric models are significantly improved to include the cloud cover as a variable.

In addition to the uncertainties in the climatic effects of CO_2, the cooling effect of aerosols suggested by McCormick and Ludwig may not be correct. Charlson and Pilat[7], Atwater[8] and Mitchell[9] have shown that since aerosols absorb and scatter, they may produce warming or cooling, depending on the ratio of absorption to scattering.

Thus, it is clear that considerably more work on the complex problem of modeling the atmosphere and on the optical properties of aerosols is needed before the long term effects of man-made pollution can be predicted. Since these problems will not be solved in the near future, it is important to initiate global measurements of aerosols on a continuous basis to monitor any changes.

We have shown in earlier theoretical studies[10] that it should be possible to make satellite observations of the aerosol optical thickness of the atmosphere from contrast measurements of ground features, and from radiance measurements. The launch of ERTS-1 offered the opportunity of investigating these theoretically derived relationships with actual satellite data. For convenience in comparing data at different wavelengths we shall refer to aerosol content as well as aerosol optical thickness. The aerosol content is defined in terms of the Elterman 1964 model vertical aerosol optical thickness; i. e., the aerosol content is given by the ratio (measured aerosol optical thickness at wavelength λ/model aerosol optical thickness at wavelength λ). The aerosol optical thickness can be related to the mass loading of the aerosols using the relationship given by Griggs[11].

These relationships were investigated using MSS data at two test sites, with ground truth being obtained with ground-based Volz photometer measure-

ments of the aerosol content. The two test sites were at San Diego, where radiance measurements over the ocean were conducted, and at the Salton Sea/ desert region, where radiance and contrast measurements were made. The test sites are illustrated with ERTS imagery in Fig. 1-1 and 1-2.

Figure 1-1. San Diego Test Site
ERTS MSS 6 Data 1-18-73

Figure 1-2. Salton Sea/Desert Test Site
ERTS MSS 5 Data 12-30-72

2. APPROACH

The approach to the investigation has been an empirical one based on theoretical calculations for model atmospheres. To make the computations manageable, certain approximations about several parameters, such as the aerosol size distribution and the underlying surface reflectance, have to be made. Hence, in the real atmosphere, model conditions are never realized, so that deviations from the theoretical relationships are expected. Thus, an empirical investigation has been conducted using the theory to provide insight into the extremes of values which may be encountered.

The two relationships studied have been one between radiance over water surfaces and the aerosol content, and another between the water/desert contrast and the aerosol content. The satellite radiance measurements were obtained from the ERTS-1 digital data, and the ground-truth measurements of the aerosol content were made with a Volz photometer at the time of selected ERTS overpasses.

The theory and its limitations are discussed in the following sections.

2.1 Relationship of Radiance and Aerosol Content

Calculations of the radiance backscattered from the earth-atmosphere system, as seen from space have been published by Plass and Kattawar.[12, 13] These calculations, using Monte Carlo techniques, consider multiple scattering of all orders, and take into account aerosol scattering and ozone absorption. Examination of the results of Plass and Kattawar shows that the outgoing radiance varies with aerosol content, and is most sensitive when the underlying surface albedo is low. The ocean, which covers much of the earth, has a low albedo at high sun angles and provides a suitable underlying surface for aerosol measurements. The calculations also indicate that the longer wavelengths are more sensitive to aerosol changes. At shorter wavelengths the

Rayleigh optical thickness is comparable to, or greater than, the aerosol optical thickness, so that changes in the aerosol content have less effect. The results obtained by Plass and Kattawar for 0.7 μm and zero albedo are plotted in Fig. 2-1.

In order to further investigate the effect of aerosols on the upward radiance over a calm water surface, Plass and Kattawar[14] made some special calculations for us under our Contract NAS1-10466, for several aerosol vertical distributions. The calculations showed a result of great importance for satellite observations of the upward radiance: the upward radiance depends strongly on the total number of aerosols, but not on their vertical distributions. Thus measurements of the upward radiance can be directly related to the total vertical aerosol content and hence the global loading.

The three wavelengths (0.7 μm, 0.9 μm and 1.67 μm) considered show comparable sensitivity to aerosol changes. However, the relative normalized radiance is less at the longer wavelengths, and since the incoming solar flux decreases at longer wavelengths the absolute radiance level decreases rapidly with increasing wavelength (the absolute radiance at 1.67 μm is about 6% of that at 0.7 μm).

The results for 0.7 μm are plotted in Fig. 2-2 to show the relationship between the upward radiance, normalized to unit incident solar flux, and the aerosol content of the atmosphere for various sun angles. A simple linear relationship is shown to exist between radiance and the aerosol content. These straight lines are based on only two values of aerosol content, but a linear relationship may be established by considering the four data points for zero albedo in Fig. 2-1. From these curves a knowledge of the sun angle and the absolute radiance at 0.7 μm allows the aerosol content of the atmosphere to be determined. From Fig. 2-2 it is seen that a 1 percent change in radiance is equivalent to about 1.5 percent change in aerosol content.

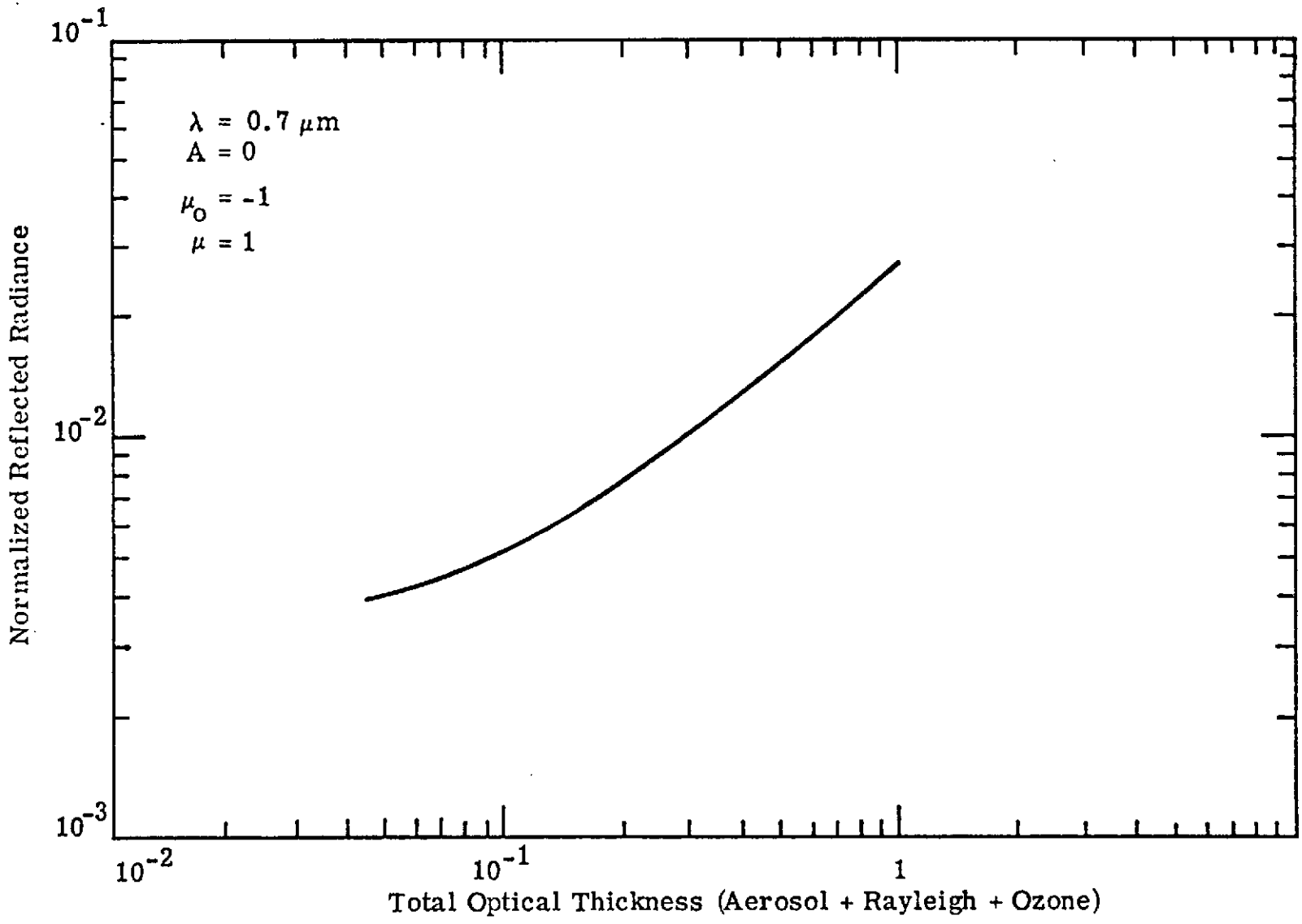

Figure 2-1. Upward Radiance vs. Optical Thickness for A = O

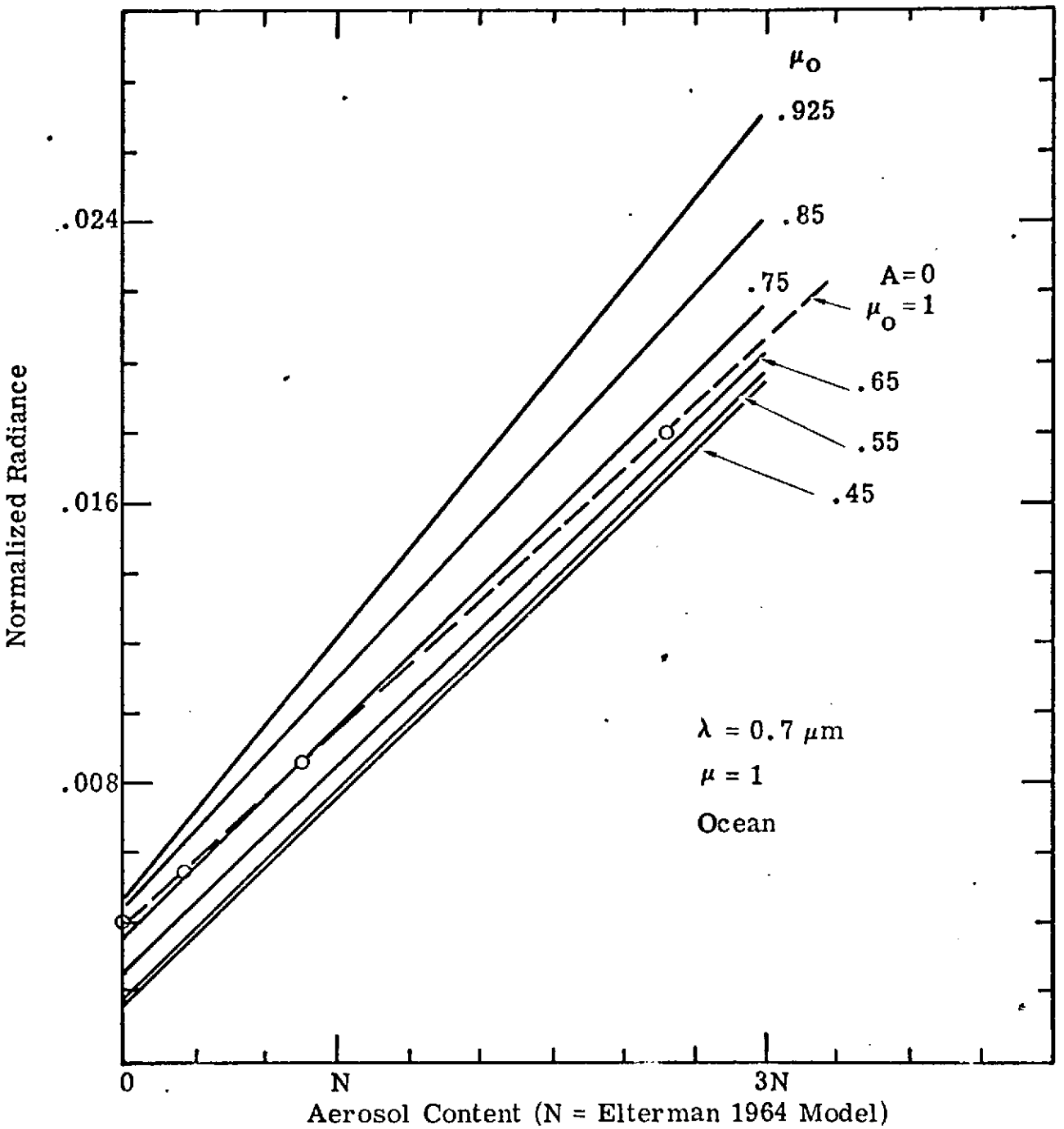

Figure 2-2. Normalized Radiance vs. Aerosol Content for 0.7μm

The data in Fig. 2-2 may be used to compute the radiance in the MSS channel 6, centered at 0.75 μm, by interpolation of the results of Plass and Kattawar at wavelengths 0.4 μm, 0.7 μm, 0.9 μm and 1.67 μm, and by assuming a rectangular spectral response 0.1 μm wide. The results, which neglect the oxygen absorption in this band, are shown in Fig. 2-3.

2.2 Relationship of Contrast and Aerosol Content

The theory of contrast reduction developed by Duntley[15] is briefly discussed below. The inherent contrast of an object relative to the background is defined as

$$C_o = \frac{B_o - B'_o}{B'_o} \tag{2-1}$$

where B_o and B'_o are the radiances of the object and background, respectively. The apparent contrast, as viewed from range, R, is defined as

$$C_R = \frac{B_R - B'_R}{B'_R} \tag{2-2}$$

where B_R and B'_R are the corresponding radiances observed at R. Duntley shows that an object of radiance B_o viewed through a scattering atmosphere with an optical depth, τ, has an apparent radiance, B_R, given by

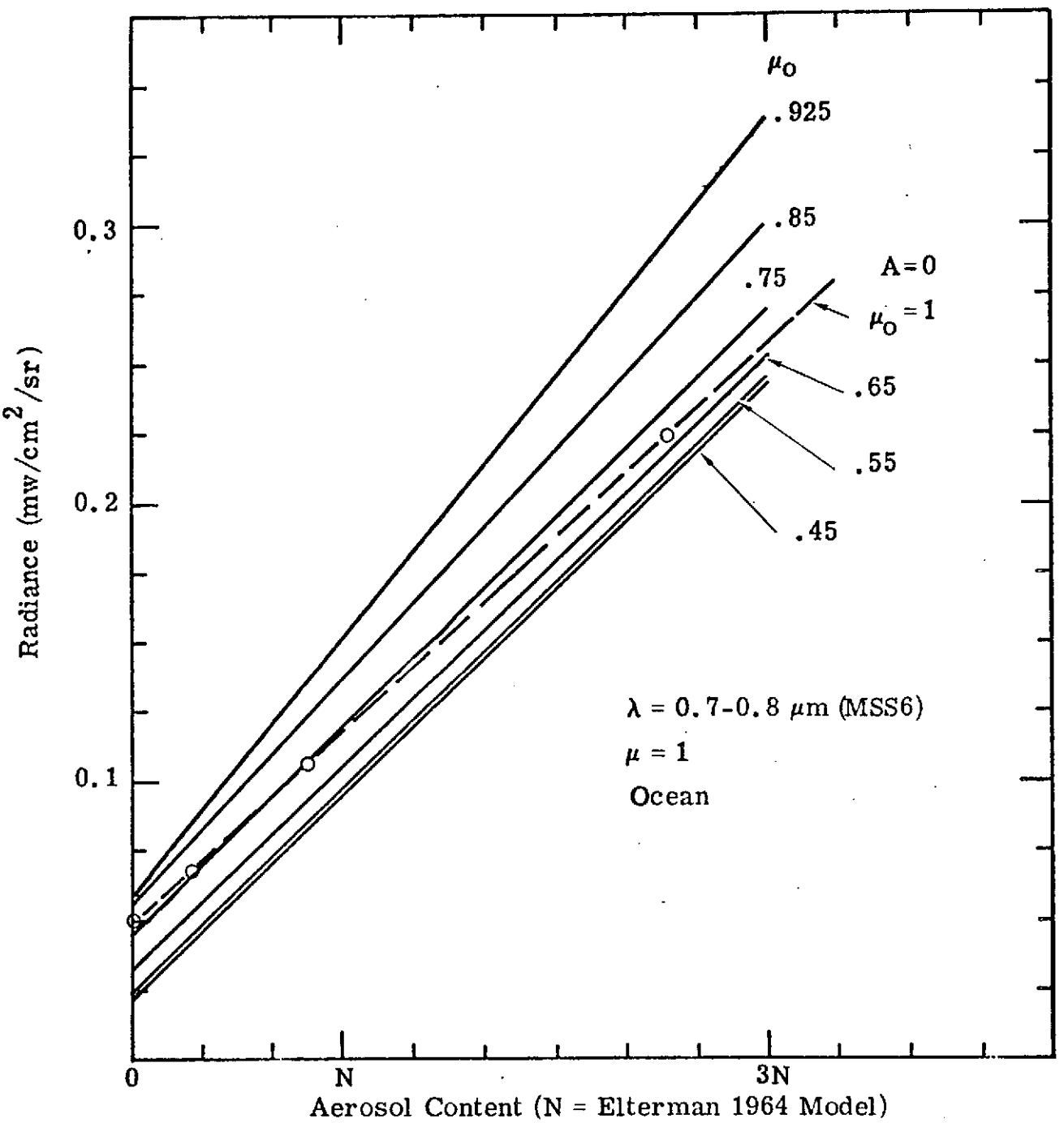

Figure 2-3. Radiance vs. Aerosol Content for MSS 6

$$B_R = B_o\, e^{-\tau} + \frac{B_a(0)}{\sigma_o}\,[1 - e^{-\tau}] \quad , \tag{2-3}$$

in which the second term on the right results from scattering into the line of sight, where $B_a(0)$ is the scattered radiance from unit thickness of the atmosphere near the object, and σ_o is the atmospheric extinction coefficient near the object.

Hence the contrast ratio C_R/C_o is found to be

$$\frac{C_R}{C_o} = \frac{1}{1 + \frac{B_a(0)}{\sigma_o B_o'}\,(e^{\tau} - 1)} \tag{2-4}$$

We fitted this equation with values of C_R/C_o calculated for the results of Plass and Kattawar[12] and the values of $B_a(0)/\sigma_o B_o'$ obtained were strongly dependent upon τ. The inapplicability of Eq. 2-4 to the case of observations made through the entire atmosphere is not unexpected, since the variation of τ is due to the particulate component only while the Rayleigh component remains constant.

A perfectly arbitrary generalization of Eq. 2-4 is made:

$$\frac{C_R}{C_o} = \frac{1}{1 + g(\tau, A)} \tag{2-5}$$

where A is the underlying surface albedo (assumed Lambertian). From values published by Plass and Kattawar for reflected radiance versus albedo, it was found that the reflected radiance is well represented by a linear function of A:

$$R_{refl}(\tau, A) = R_{refl}(\tau, O) + A[R_{refl}(\tau, 1) - R_{refl}(\tau, O)] \quad . \tag{2-6}$$

The apparent contrast is, consequently:

$$C_R = \frac{R_{refl}(\tau, A) - R_{refl}(\tau, A')}{R_{refl}(\tau, A')}$$

$$= \frac{(A-A')\,[R_{refl}(\tau, 1) - R_{refl}(\tau, O)]}{R_{refl}(\tau, O) + A'[R_{refl}(\tau, 1) - R_{refl}(\tau, O)]} \quad . \tag{2-7}$$

where A and A' are the albedos of the object and background respectively.

Since

$$C_o = \frac{A - A'}{A'} \tag{2-8}$$

we have

$$\frac{C_o}{C_R} = 1 + \frac{R_{refl}(\tau, O)}{A'[R_{refl}(\tau, 1) - R_{refl}(\tau, O)]} \quad . \tag{2-9}$$

By identifying with Eq. 2-5 we find that the unspecified function $g(\tau, A)$ may be separated into τ- and A-dependent parts:

$$g(\tau, A) = f(\tau)/A \tag{2-10}$$

where

$$f(\tau) = \frac{R_{refl}(\tau, O)}{R_{refl}(\tau, 1) - R_{refl}(\tau, O)} \quad . \tag{2-11}$$

Values $f(\tau)$ using Eq. 2-11 have been calculated for the center wavelengths of three of the four MSS channels, based on interpolation of values of $R(\tau, O)$ and $R(\tau, 1)$ calculated by Plass and Kattawar,[12, 13, 14] for the wavelengths 0.4 μm, 0.7 μm, 0.9 μm and 1.67 μm. The results, for

three sun angles, are shown in Figs. 2-4, 2-5, and 2-6. The fourth MSS channel between 0.8 μm and 1.1 μm is not considered due to the strong absorption by water vapor, which is an atmospheric variable, in this band. The function $f(\tau)$ is related to the experimentally observable quantities C_o, C_R and A' by Eq. 2-5 and 2-10:

$$f(\tau) = A'(C_o/C_R - 1) \quad . \tag{2-12}$$

Thus, a measurement of the contrast ratio and knowledge of albedo and sun angle yields a value of $f(\tau)$ that determines τ.

The preceding analysis is based on calculations using a Lambertian underlying surface. Of course, in practice this type of surface does not exist, and reflectivity should be used instead of albedo in determining $f(\tau)$ from Eq. 2-12. The reflectivities of natural surfaces vary with wavelength and sun angle and are not accurately known. A relatively simple case is the Salton Sea/desert contrast. However, the reflectivity of sand which has been measured for certain conditions by Coulson[16, 17] cannot be deduced for all the conditions required for this program. The radiance reflected from water is more readily calculated,[18] but varies with surface conditions and suspended matter. Thus, due to the shortcomings of the available reflectance data, and to the approximations in the theory, the empirical approach must be used.

2.3 Potential Problem Areas

The discussions in Sections 2.1 and 2.2 are based on theoretical calculations which use a model atmosphere, model aerosol properties, and assume a smooth water surface or a Lambertian surface. Since these model conditions are never realized in practice, empirical relationships

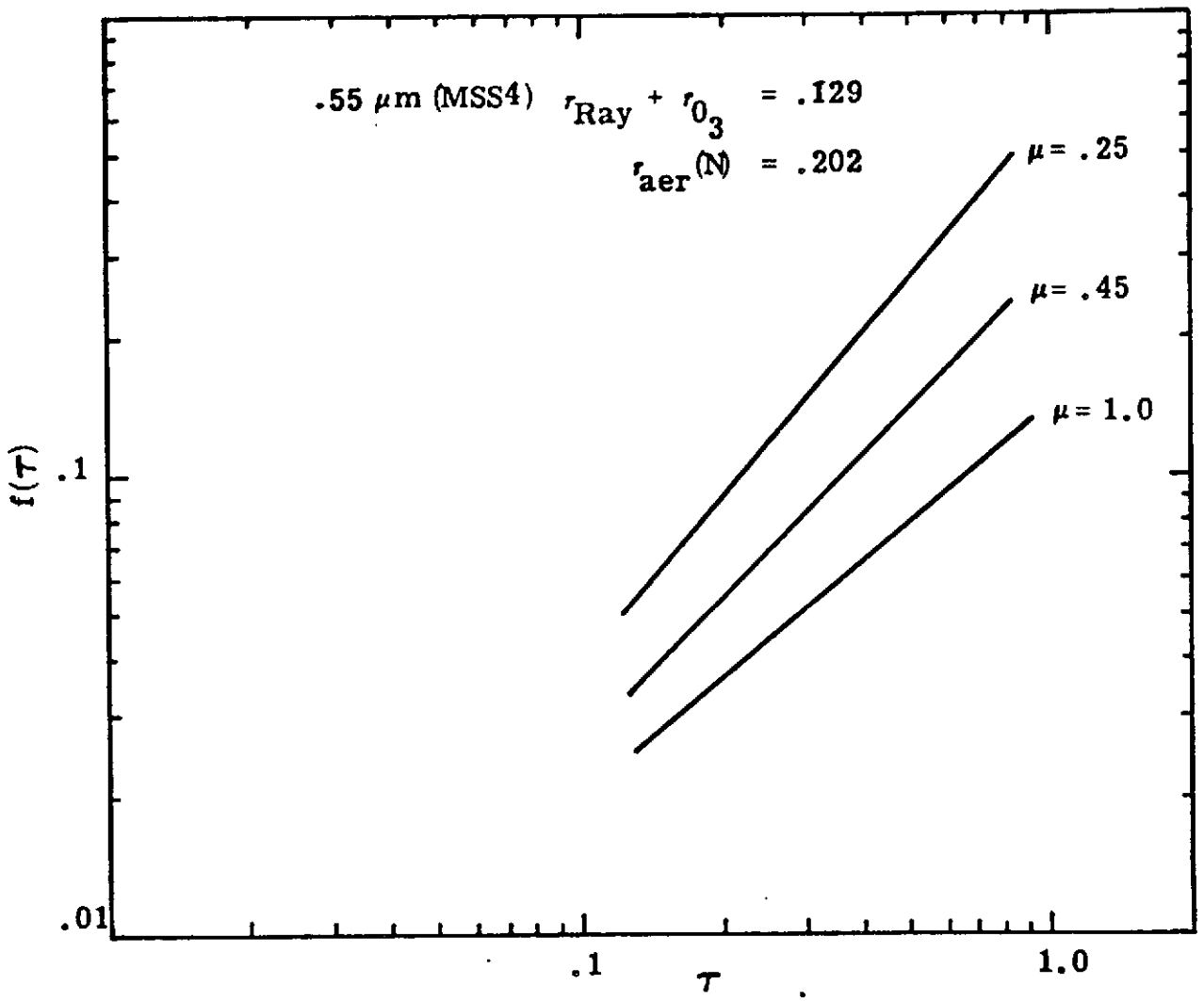

Figure 2-4. f (τ) vs τ for three sun zenith angles, θ, (μ = cos θ) (MSS4)

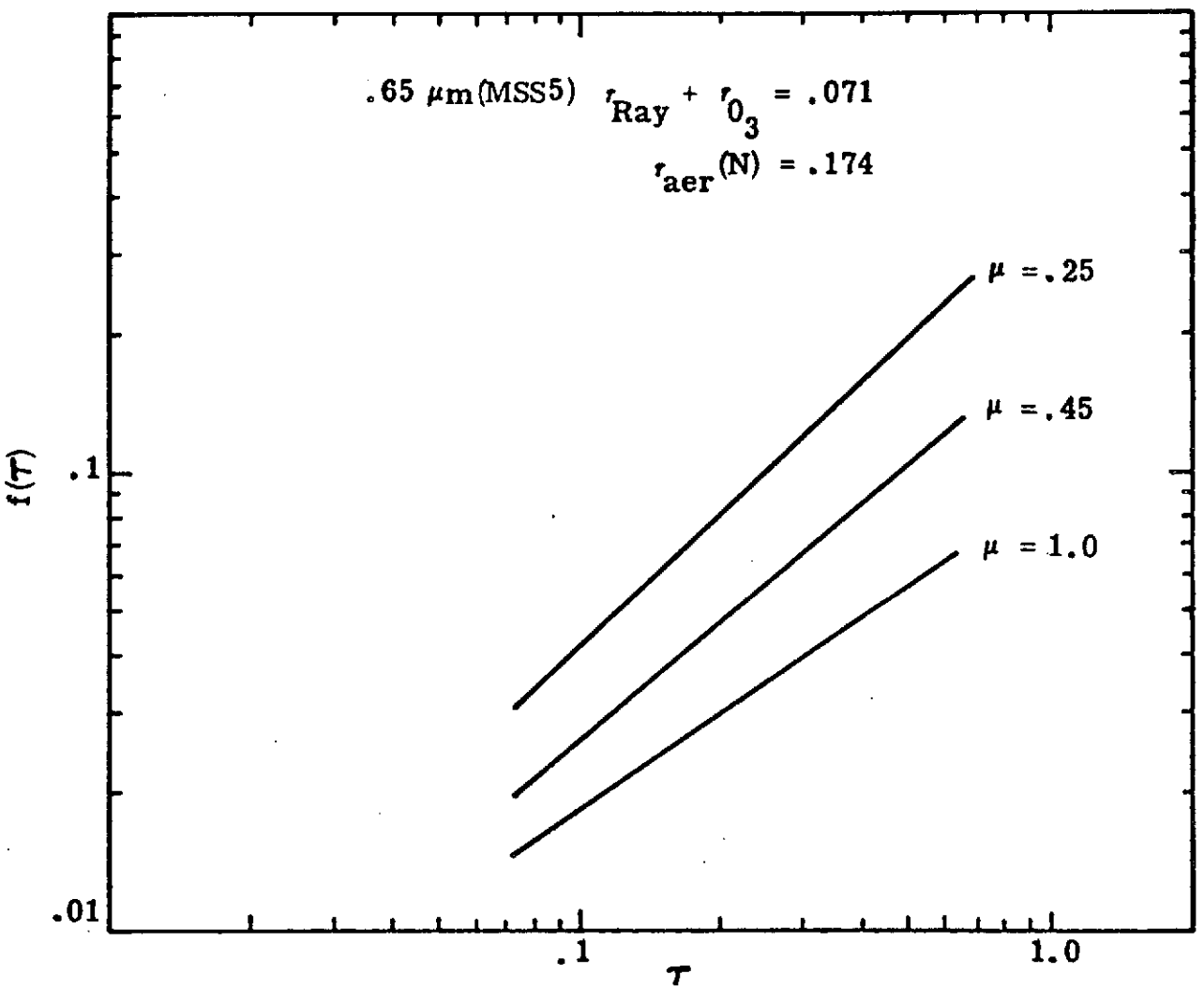

Figure 2-5. f (τ) vs τ for three sun zenith angles, θ, (μ = cos θ) (MSS5)

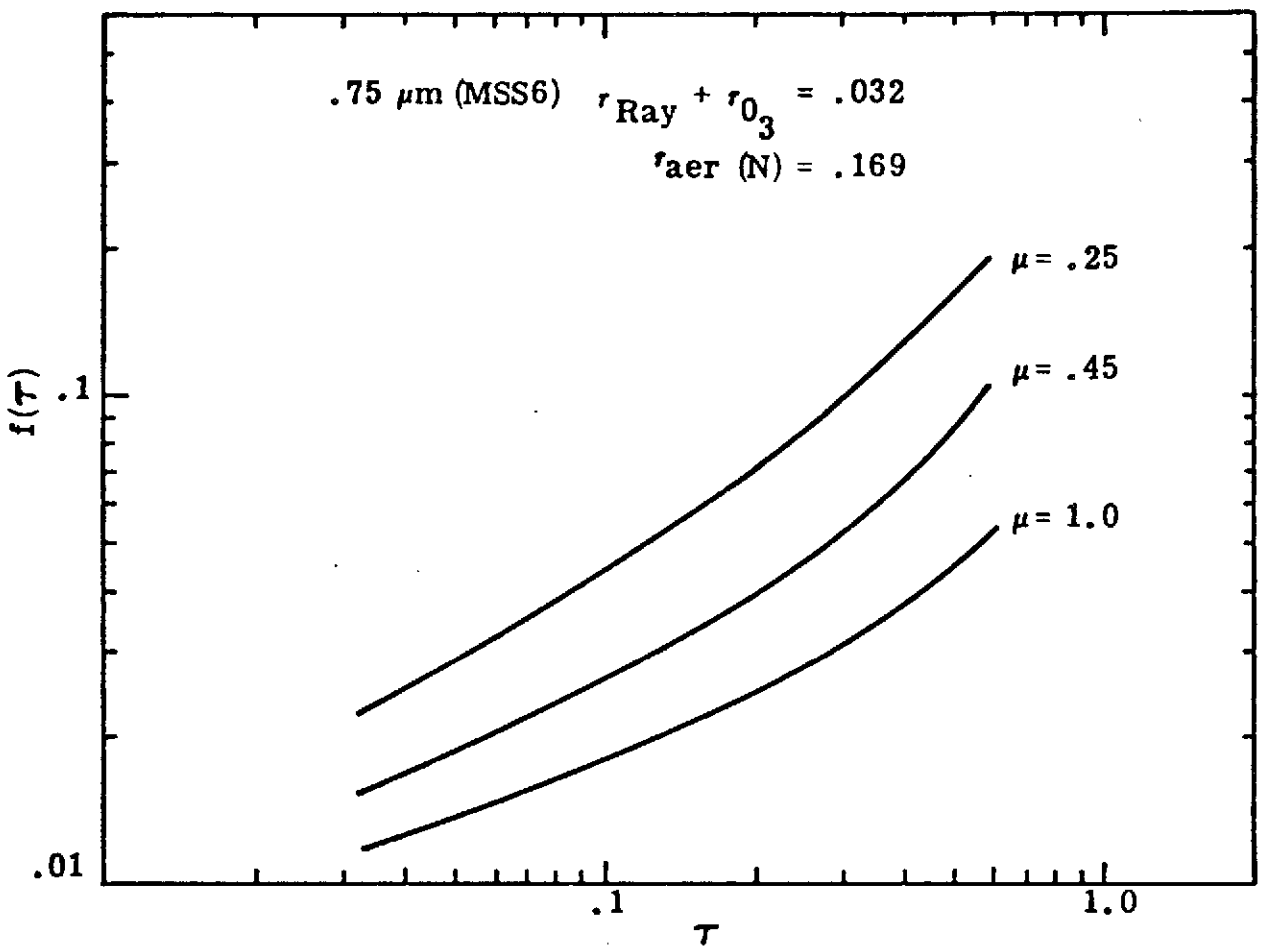

Figure 2-6. f (τ) vs τ for three sun zenith angles, θ, (μ = cos θ) (MSS6)

between the satellite data and the aerosol content have been investigated. However, two potential problems must be considered, although as shown later in the discussion of the results, they do not appear significant.

2.3.1 Sun Glitter

If the ocean were perfectly smooth as assumed in the calculations an image of the sun would be seen at the specular reflection angle, and the only upwelling surface radiation observable at other look angles from space would be the diffuse sky radiation reflected from the ocean surface and the radiation scattered up from below the ocean surface. As the smooth ocean surface is increasingly disturbed, a glitter pattern becomes increasingly larger about the specular point. At sun zenith angles greater than about 30^{o} the glitter effect has been considered negligible (except for very rough seas) at the nadir point. However, measurements by Hovis (private communication from R. Fraser) suggest that this assumption is not correct, so that the ocean surface radiance at the nadir is not known accurately.

This problem might be overcome by making observations at two wavelengths, assuming that the spectral variation of the surface radiance is known. The choice of wavelengths must be made carefully since the spectral distribution of the radiance does vary due to ocean properties such as chlorophyll content, suspended matter and depth.

2.3.2 Surface Reflectance Gradients

The calculations of Plass and Kattawar which are used in deriving the contrast attenuation relationship in Section 2.2 assume an underlying surface of constant reflectivity extending to infinity. However, for the contrast measurements there are two adjacent surfaces of different reflectivities, and radiation reflected from one surface is scattered into the atmosphere above the other surface so that the apparent radiance above that surface is different from the calculated theoretical value.

3. DATA ANALYSIS METHODS

The investigation has utilized the radiances measured by the MSS, and the aerosol content measured by ground-based observations with a Volz photometer at the time of several ERTS overpasses. Aircraft measurements were also made of the Salton Sea/desert inherent contrast, but these data have not yet been received for analysis.

3.1 ERTS Data

The data for the four MSS channels have been received as bulk processed black and white 9.5 in positive prints and transparencies, and as bulk processed digital 7-track computer compatible tape, selectively ordered after viewing the black and white products.

The transparencies of the first sets of data received were analyzed with a Jarrell-Ash microdensitometer to obtain the radiances at selected areas of the test sites. It was readily apparent that the photographic data were not accurate enough, as expected, for this investigation. On several transparencies, for instance, the density of the transparency over a water surface was greater than that of the blackest step in the calibration grey scale, which corresponds to zero radiance. No such obvious errors were found in the digital data, and all the results given in this report are based on the digital data.

To extract the radiance data from the computer compatible tapes (CCT), a program was written to read data in prescribed geographical areas from the tapes on a CDC 6400. The areas of interest for analysis were chosen by viewing the black and white products, and selecting areas within the test sites free of obvious clouds, or effluents in the water. The location of typical selected areas, about 6 km on a side, are shown for each test site in Fig. 3-1. The word counts are printed out for each area,

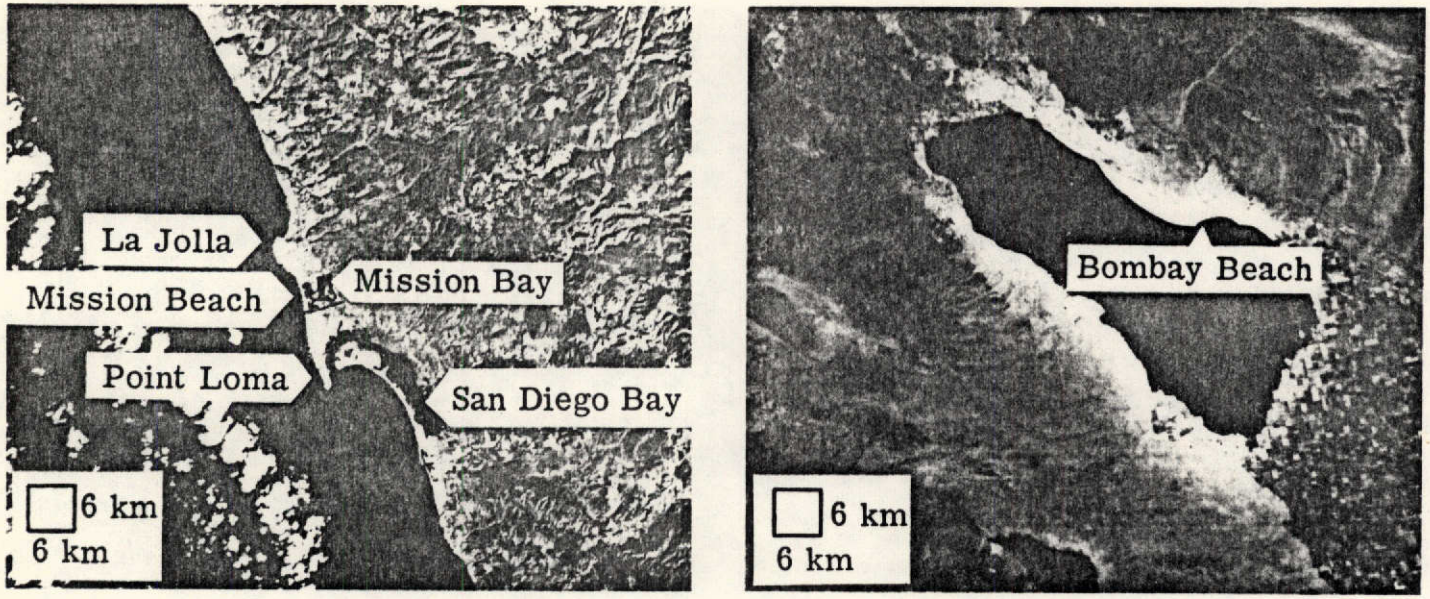

(a) San Diego Test Site

(b) Salton Sea Test Site

Figure 3-1. Location of Analysis Areas

and can be converted to radiance using the calibration data given in the ERTS Data Users Handbook. The radiance is proportional to the word count in each channel, with the radiance per count being given by .0195, .0157, .0139 and .0730 mw/cm^2/sr for MSS 4, 5, 6 and 7 respectively.

To analyze the Salton Sea/desert data within one of the selected areas, two smaller areas about 300m x 300m are chosen, one on the water surface and another on the desert. The water area is selected away from the shoreline where the radiance is essentially uniform within the area, and the desert area is selected for high radiance and uniformity. An average radiance for each area is estimated for each MSS band.

The San Diego data are analyzed in a similar fashion, although only the water surfaces are of concern. The mean radiance for each MSS band is estimated for small areas of the ocean just off the coast, and of the various bays in the San Diego area.

3.2 Ground-Truth Measurements

Measurements of the aerosol content were made with a Volz sun photometer at times of selected ERTS overpasses at the Salton Sea/desert site, and at every overpass at San Diego as weather permitted.

The Volz photometer has been widely used[19] to measure the turbidity of the atmosphere on cloudless days. It consists of a lens, a photocell, a pivoted scale, a microammeter, and a level. When the instrument is level, the relative atmospheric path length (in air mass units) can be read directly from the pivoted scale. The instrument is then directed toward the sun and the radiance recorded. The solar energy enters the instrument through the lens whose focal length is 4.5 cm. A diaphragm limits limits the angular field to about one degree. A bandpass filter limits the wavelength region to 0.5 ± 0.06 micron. Before the radiation reaches the photocell, it is diffused by a ground glass plate mounted

directly behind the diaphragm. The narrow field of view used in looking at the small, bright source excludes nearly all scattered air light from the instrument, thus the aerosol optical thickness, τ_A, can be determined from

$$J = \frac{J_o}{F} \exp\left[-(\tau_R + \tau_o + \tau_A)\, m\right] \qquad (2\text{-}13)$$

where τ_R and τ_o are the optical thicknesses due to pure Rayleigh scattering and ozone absorption, respectively, at $\lambda = 0.5$ micron and air mass, m, of 1. We use the values of Elterman[20] who gives $\tau_R = 0.145$ and $\tau_o = 0.012$. These values disagree only slightly with those used by Flowers, et al.[19] who listed values as $\tau_R = 0.146$ and $\tau_o = 0.0092$. The quantities J and J_o in Eq. 2-13 are the Volz photometer deflections, which are proportional to the observed solar intensity and the solar energy outside the atmosphere (air mass = 0), respectively. F is the sun-earth distance correction factor. The quantity J_o is determined by measuring J over a wide range of air masses during periods when the aerosol optical thickness, τ_A, remains constant, and extrapolating to zero air mass. Calibrations of our Volz photometer several times over recent years have shown good repeatability.

It was originally planned to use an Exotech radiometer to supplement the Volz measurements; the Exotech instrument has four channels with approximately the same spectral response as the ERTS MSS channels. Unfortunately the Exotech design does not lend itself readily to sun observations (it was designed for downward-looking aircraft measurements), and no satisfactory data were obtained during the program. The first version of the instrument did not have baffles between the lenses and the detectors, so that too much scattered sky radiation was falling on the detectors. This problem was corrected by the manufacturer. However, it was found impossible to get good repeatable readings when pointing at the sun, without

significant redesign of the sighting optics and readout of the instrument, which was not done, and no useful data were obtained.

3.2.1 Aircraft Measurements

In order to determine the inherent contrast on the Salton Sea/ desert test site, two flights with the NASA C130 aircraft were planned. Unfortunately, the first flight scheduled for 12-12-72 was cancelled due to a failure of the aircraft MSS, and the next flight which took place on 4-9-73 produced no useful data due to considerable cloud cover. Another flight was scheduled for, and took place on, 5-23-73 in excellent clear sky conditions. It was not possible, due to other priorities for the aircraft, to schedule another flight before the end of this program.

The preliminary aircraft photographic data for the 5-23-73 flight were received and reviewed, and the digital data on computer compatible tapes were requested 6-26-73. Unfortunately these digital data had not been received at the conclusion of this program on 10-6-73, so that no aircraft measurements are available as ground truth.

4. RESULTS

Significant results were obtained in analyzing the ERTS digital data and the ground-truth measurements. A linear relationship, as predicted by theory, was found to exist between the MSS radiances over water surfaces and the aerosol content of the atmosphere. A linear relationship was also found between the contrast function $(C_o/C_R - 1)$ and the aerosol content.

4.1 Volz Data

During the program there were twenty-two ERTS overpasses at each of the test sites. Six trips were made to the Salton Sea/desert test site to make ground-truth measurements, and data were obtained on five occasions; cloud cover prevented the taking of data on just one occasion. It was planned to make Volz photometer measurements for each overpass at San Diego, but the overpasses coincided with cloud cover with surprising frequency, and data were obtained on only five occasions. The Salton Sea ground-truth measurements were always made on the shoreline at Bombay Beach on the east side of the sea. The San Diego observations were made in different locations each time, but always close to the ocean.

The results of the measurements are given in Fig. 4-1, and show that in general the aerosol content was less than the value given by Elterman[21] in his 1964 model atmosphere (Elterman's model aerosol distribution corresponds to a 25 km visibility at the surface). The measurements on a few of the days show quite rapid changes, which are greater than the instrument error. They could possibly be due to the movement of undetected thin clouds between the sun and the observer, although all these variable measurements were taken in apparently completely clear sky conditions. The variations are probably due to the movement of air cells with different aerosol content in the lower atmosphere.

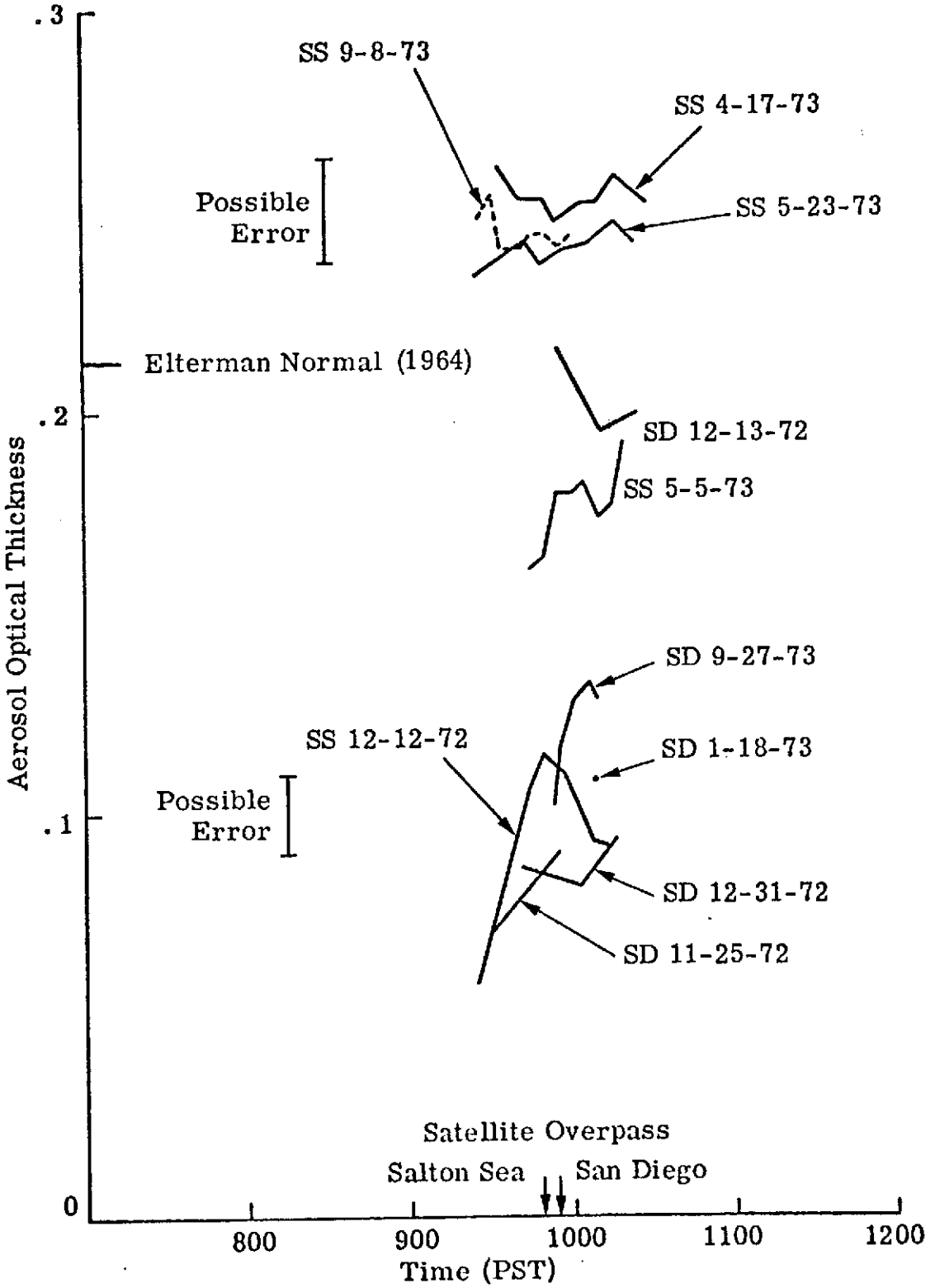

Fig. 4-1. Volz Data

4.2 ERTS Radiance Measurements

Although ten sets of ground-truth data were obtained at the two test sites, the ERTS digital data for only eight of these were received before the end of the program. These data, given in Tables 4-1 and 4-2, together with a single point provided by Fraser[22] in the Atlantic (see Table 4-3), are used to investigate the radiance-aerosol content relationship, and the contrast-aerosol content relationship. The radiance values for MSS 7 are not listed in the tables, since they are low and inaccurate over water surfaces, being close to the instrument noise level (see Section 4.3.2). In addition, the radiance in this channel is influenced by the variable atmospheric water vapor content.

4.2.1 Radiance-Aerosol Relationship (Water Surface)

The investigation of the radiance-aerosol relationship over water surfaces is based on eight data points, four over the Pacific at San Diego, three over the Salton Sea, and one over the Atlantic off the coast of North Africa, where measurements of the aerosol content are available. The radiance values are normalized to a sun angle of $\mu = 0.45$, using a correction based on the theoretical variation with sun angle given in Fig. 2-3; it is assumed that the correction is the same for each channel. The correction is greater than 5% only for the three points with high sun angle.

The normalized radiances for all four MSS channels are plotted against the aerosol content in Fig. 4-2. It is seen that, as predicted by theory, a linear relationship exists for all four channels, being best for MSS 5 and MSS 6. MSS 6 shows excellent agreement with the theoretical relationship shown in Fig. 2-3, suggesting that the model is very reasonable, particularly for zero aerosol content (i.e., a pure molecular atmosphere). The results for MSS 7 are given only to illustrate the low radiance values discussed above, and even though a linear relationship is indicated,

TABLE 4-1. Radiance ($mw/cm^2/\mu m/sr$) Data for San Diego Test Site

Date	Sun Angle (μ)	Volz Aerosol Content	MSS Channel	La Jolla Ocean Radiance	Mission Beach Ocean Radiance	Point Loma Ocean Radiance	Mission Bay Radiance	San Diego Bay Radiance
11-25-72	0.52	0.42 N	4	2.92	3.32	3.51	3.32	3.51
		(Pt. Loma)	5	0.95	1.10	1.10	1.10	1.26
			6	0.42	0.47	0.44	0.42	0.51
12-13-72	0.47	1.01 N	4	3.32	Cloud	Cloud	Cloud	Cloud
		(La Jolla)	5	1.42				
			6	0.69				
12-31-72	0.45	0.39 N	4	3.12	3.12	3.12	3.22	3.12
		(La Jolla)	5	0.95	1.03	0.95	1.18	1.18
			6	0.42	0.42	0.42	0.55	0.55
1-18-72	0.47	0.51 N	4	2.92	3.42	3.51	3.61	3.51
		(La Jolla)	5	1.00	1.26	1.26	1.42	1.42
			6	0.42	0.55	0.49	0.62	0.55

TABLE 4-2. Radiance ($mw/cm^2/\mu m/sr$) Data for Salton Sea/Desert Test Site

Date	Sun Angle (μ)	Volz Aerosol Content	Inferred Aerosol Content	MSS Channel	Radiance		Apparent Contrast C_R
					Salton Sea	Desert	
12-12-72	0.47	0.54 N	0.64 N	4	2.90	9.20	2.2
				5	1.10	8.30	6.5
				6	0.55	6.50	10.7
4-17-73	0.82	1.19 N	1.19 N	4	4.68	15.8	2.4
				5	2.20	15.9	6.2
				6	1.11	12.5	10.3
5-5-73	0.87	0.77 N	1.46 N	4	5.23	17.5	2.1
	(Effluents present in water)			5	2.68	16.6	4.1
				6	1.53	13.4	6.4
5-23-73	0.88	1.11 N	1.05 N	4	4.87	18.1	2.7
				5	2.42	18.3	6.6
				6	1.21	14.3	10.9
8-26-72	0.82		0.98 N	4	4.20	14.6	2.5
				5	2.05	14.5	6.1
				6	1.04	11.1	9.7
9-13-72	0.77		1.18 N	4	3.70	14.0	2.8
				5	1.80	13.9	6.7
				6	1.07	11.1	9.4

Table 4-2 continued...

Date	Sun Angle (μ)	Volz Aerosol Content	Inferred Aerosol Content	MSS Channel	Radiance Salton Sea	Radiance Desert	Apparent Contrast C_R
10-1-72	0.72		1.12 N	4	3.90	14.8	2.8
				5	1.70	13.4	6.7
				6	0.97	10.3	9.6
11-6-72	0.57		0.91 N	4	3.90	12.9	2.3
				5	2.00	11.8	4.9
				6	1.20	9.1	6.6
11-24-72	0.52		0.73 N	4	3.12	10.3	2.3
				5	1.29	9.8	6.6
				6	0.60	8.0	12.5
12-30-72	0.45		0.52 N	4	2.83	9.45	2.4
				5	1.10	8.90	7.1
				6	0.49	7.10	13.6
1-17-73	0.47		0.53 N	4	3.12	9.35	2.0
				5	1.11	8.98	6.1
				6	0.55	6.92	11.5
3-30-73	0.75		1.08 N	4	4.38	15.2	2.5
				5	2.12	15.1	6.1
				6	1.01	11.9	12.2

TABLE 4-3. Radiance ($mw/cm^2/\mu m/sr$) Data for Atlantic Ocean ($21^{o}N$, $17^{o}W$) [22]

Date	Sun Angle (μ)	Volz Aerosol Content	MSS Channel	Radiance
8-9-72	0.86	2.33 N	4	5.52
			5	3.18
			6	2.04

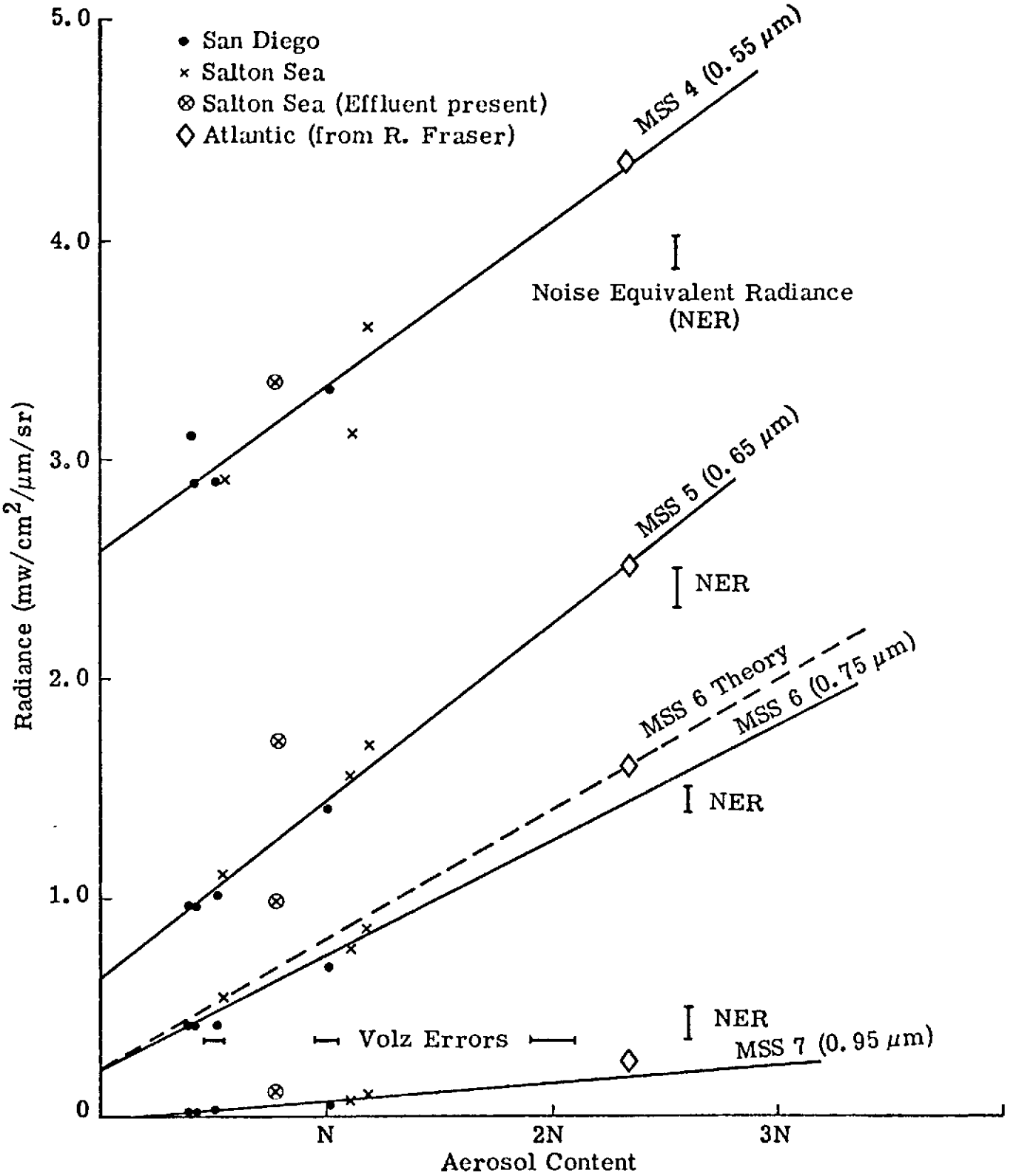

Fig. 4-2. Radiance vs. Aerosol Content Over Water Surfaces (Normalized to sun angle $\mu = .45$)

this channel is not considered useful for determining the aerosol content. The results for MSS 4 show more scatter of points about the mean curve than for the other channels. The reason for the larger scatter in this channel is not readily obvious, since the radiance errors are not significantly different from the other channels (see Section 4.3.2). Possibly this channel is more sensitive to changes in the water reflectance due to the presence of effluents, chlorophyll, or other suspended material in the water, although on the one occasion when effluents were obviously present in the Salton Sea, the radiance in MSS 4 was closer to the mean curve than in the other channels.

Effluents were clearly apparent on 5-5-73 when ground-truth measurements were made, and on subsequent imagery of the Salton Sea during the summer months. The effluents, which are presumably due to irrigation run-off, were not observed during the winter months, when there is more rain and it is cooler, thus requiring less irrigation. These effluents result in variable high radiances over the water surface. To analyze the data for 5-5-73, an area exhibiting the lowest values of radiance was selected, but as seen in Fig. 4-2, the radiances appear too high for the measured aerosol content, especially for MSS 5 and 6. The effluent pattern is more apparent in the photographic images at shorter wavelengths. However, the data point for MSS 4 shows less deviation from the previous data than at the longer wavelengths. In addition, the spectral variation of radiance has the same basic shape as other data. Thus, the spectral behavior of this effluent, and its effect on aerosol observations is not completely consistent, and further studies of this type of data are required. However, it is clear that care should be taken in using data from bodies of water where effluents occur on an intermittent basis. The data may be readily screened by visual examination of the photographic images.

4.2.2 Radiance-Aerosol Relationship (Desert Surface)

The theory discussed in Section 2 showed that the radiance over high albedo surfaces is not very sensitive to atmospheric aerosol content changes. The data at the Salton Sea/desert test site allows this conclusion to be investigated over the desert, which has a high albedo ($\sim$ 0.3).[23] Since ground truth are available for only four ERTS overpasses, the data for several other ERTS overpasses are utilized with help of the radiance-aerosol relationship in Fig. 4-2. This linear relationship is assumed to be correct, and is used to determine the aerosol content for twelve overpasses from the Salton Sea radiance for MSS 6. The desert radiances, given in Table 4-2, are plotted in Fig. 4-3, against these inferred aerosol contents, also listed in Table 4-2. The data, uncorrected for sun angle, appear to show a good linear relationship. However, after normalizing the radiances to a sun angle of $\mu = .45$, using the theoretical variation for a Lambertian albedo of 0.3 (actually 0.4 or 0.2 which show approximately the same variation) given by Plass and Kattawar,[12] the radiance clearly shows no obvious dependence on the aerosol content, as predicted by theory. It is realized that the desert is not a true Lambertian surface, with the backscattering being greater than the forward scattering.[24] However, since it is close to being a diffuse reflector, and no significant variability of albedo with sun angle has been found,[25] it is believed that the above conclusions are not affected.

4.2.3 Analysis of Potential Problem Areas

Two potential problem areas for this program were identified in Section 2.3. The first one, sun glitter, may be discussed on the basis of the preceding radiance-aerosol content analysis, and the second, surface reflectance gradients, should be studied before analyzing the contrast-aerosol content relationship.

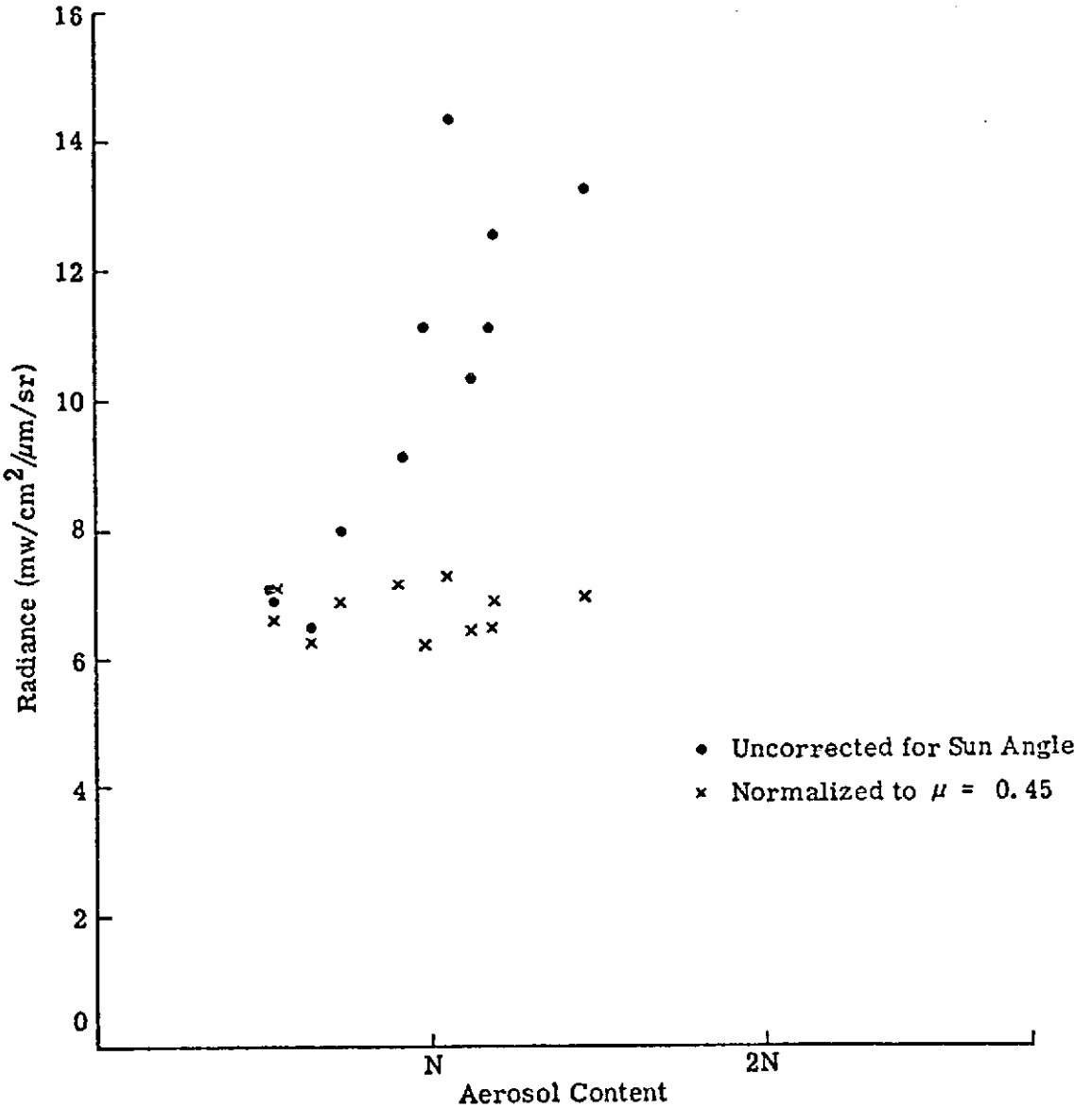

Fig. 4-3. Desert Radiance vs. Aerosol Content for MSS 6

4.2.3.1 Sun Glitter

No evidence of sun glitter has been observed in the ERTS data received during the program. (Sun glitter was observed on the photographic data from the NASA aircraft overflight at 2000 ft. altitude on 5-23-73, but was not identifiable on the ERTS data for the same time). All of the data at the San Diego and Salton Sea/desert test sites were obtained over relatively calm seas, so that the sun glitter might be expected to be minimal. However, the one data point in Fig. 4-2 for the Atlantic Ocean was obtained over rough seas, with seven foot waves and winds of about 20 knots being reported. Presumably, sun glitter should be apparent under these conditions. However, it is seen in Fig. 4-2 that this point does not significantly deviate from the linear relationships for the San Diego and Salton Sea data. Thus it is believed that nadir observations will not be significantly affected by sun glitter, although more rough sea data are needed to draw any firm conclusion.

It was suggested in Section 2.3.1 that observations at two wavelengths might be used to eliminate a sun glitter problem if it should occur. In order to investigate this possibility the spectral variations of the upwelling radiance over water surfaces have been plotted. Figure 4-4 shows the results for several ERTS overpasses at the Salton Sea. These values are not normalized, and higher radiances are expected for higher sun elevations for a given aerosol content. Within the errors of the MSS radiance measurements, there are no obvious spectral differences from one overpass to the next, at least at the MSS wavelengths. However, there appears to be a tendency at sun elevations below about 50^{o} for the radiance decrease from MSS 5 to MSS 6 to be less than at high sun elevations.

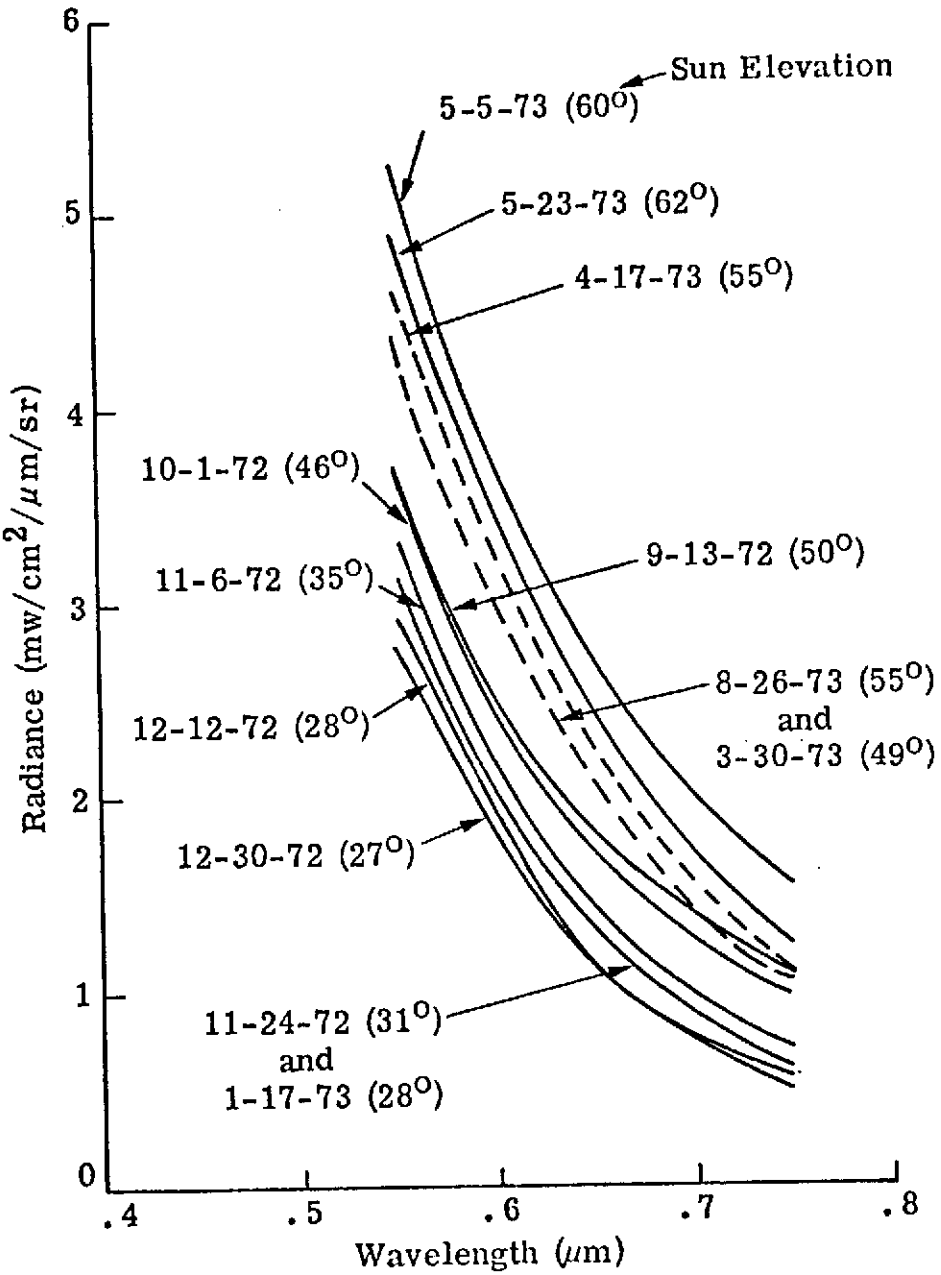

Fig. 4-4. Salton Sea Water Radiance vs. Wavelength

The data for the ocean and bays at the San Diego test site are given in Fig. 4-5, and show the same basic variations as the Salton Sea measurements. Also given in Fig. 4-5 are the data for the Atlantic Ocean provided by Fraser.[22] These radiances, which are averaged over a 20 x 20 km area show less decrease with wavelength than the San Diego and Salton Sea data. The Atlantic Ocean was rough, whereas the San Diego data, and probably all of the Salton Sea data, were for relatively calm surfaces, without whitecaps. If the difference in the Atlantic data is due to the surface roughness, then it is unlikely that a two wavelength method could be used to eliminate a sun glitter problem. However, with only one set of rough sea data, and the errors in the measurements, no conclusion can be reached at the present time.

4.2.3.2 Surface Reflectance Gradients

Examination of the digital data in the San Diego coastal regions and at the Salton Sea shows that the radiance over the water surface is higher immediately at the water-land boundary, but rapidly decreases and reaches a uniform value within about 1300 ft of the boundary. Thus, the effects of scattering from the adjacent high albedo land appears to be negligible beyond about 1300 ft from the shoreline. The water radiance data used for the preceding radiance-aerosol study and the following contrast-aerosol analysis were all obtained beyond 1300 ft from the shoreline, where the radiance was uniform.

4.2.4 Contrast-Aerosol Relationship

The Salton Sea/desert test site is used to investigate the contrast-aerosol content relationship discussed theoretically in Section 2.2 To determine the function $f(\tau)$ given in Eq. (2-12), and plotted in Figs. 2-4, 2-5, and 2-6, the value of A', the water surface reflectivity, and C_o, the

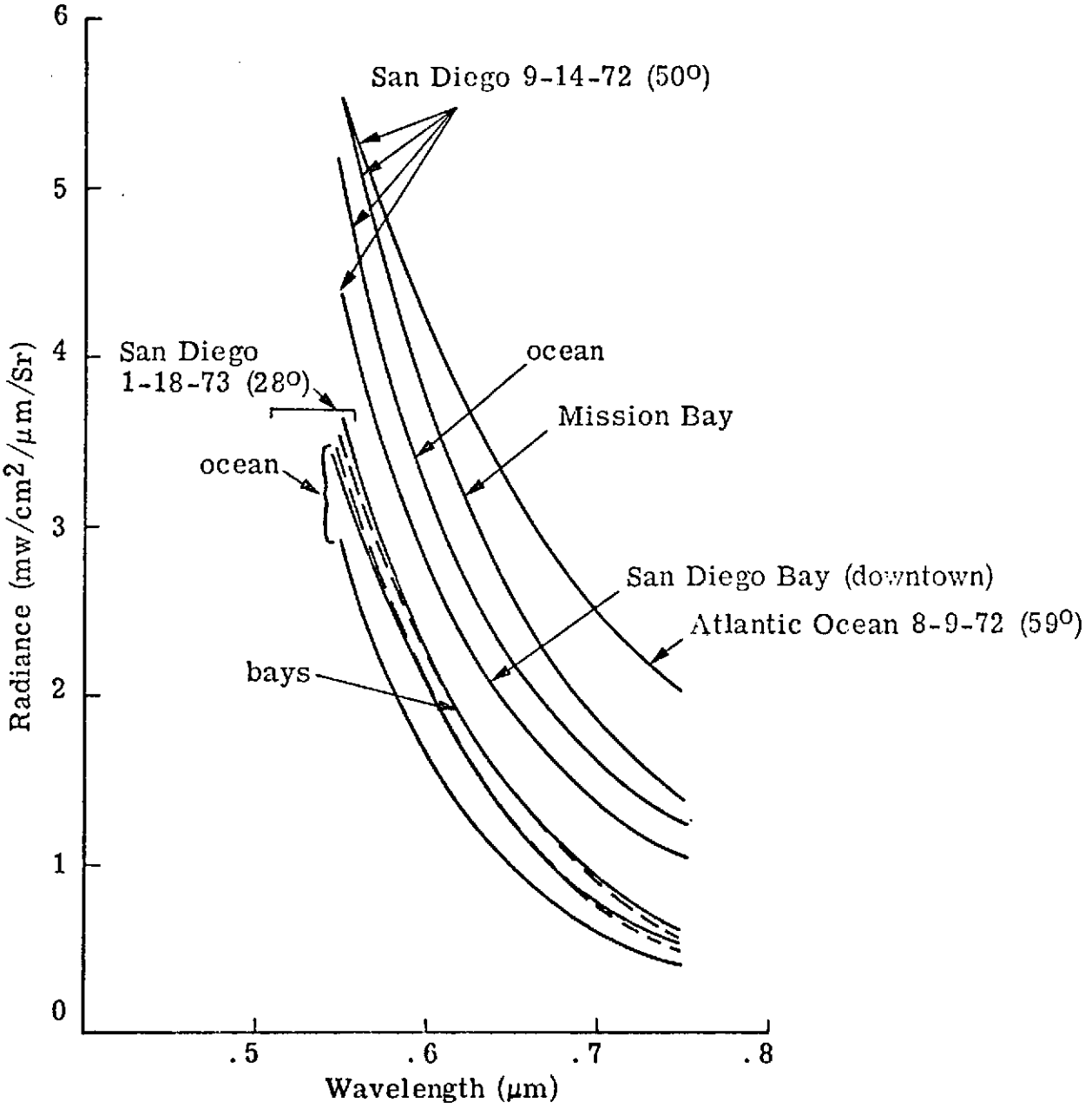

Fig. 4-5(a). San Diego and Atlantic Ocean Water Radiance vs. Wavelength

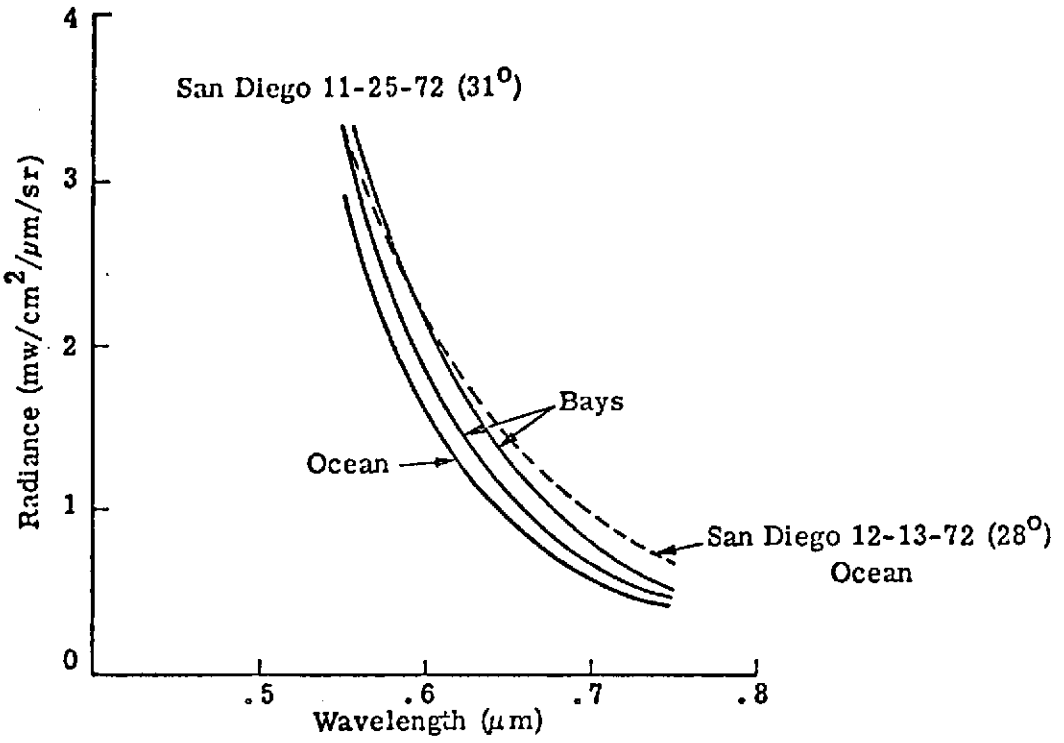

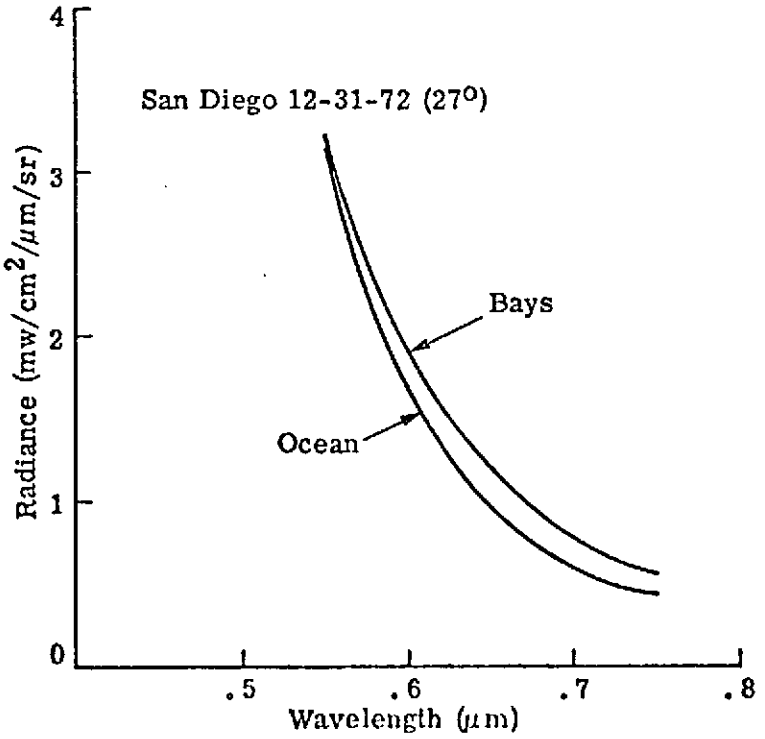

Fig. 4-5(b). San Diego Water Radiance vs. Wavelength

inherent contrast, must be known as a function of wavelength and sun angle; C_R, the apparent contrast, is calculated directly from the ERTS digital data, and is listed in Table 4-2. Since the NASA aircraft MSS data are not available to determine C_o, and A' is not known, certain approximations must be made. A' is assumed to be independent of sun angle and wavelength so that the function $(C_o/C_R - 1)$ $(= f(\tau)/A')$ is examined. C_o is estimated by assuming a reflectivity of 0.30 for the desert and 0.02 for the Salton Sea (based on albedos measured by Griggs[21]) giving a value of 14.0 for C_o. It is further assumed that C_o is independent of wavelength and sun angle.

Ground-truth measurements are available for only four ERTS overpasses at the Salton Sea/desert test site, and on one of those occasions effluents were present in the water, so that only three data points can be used. However, the data from several other ERTS overpasses are utilized with the help of the radiance-aerosol content relationship in Fig. 4-2. This linear relationship is assumed to be correct, and is used to determine the aerosol content from the Salton Sea radiance for MSS 6. These values are then treated as ground-truth values of the aerosol content.

The values of $(C_o/C_R - 1)$ are calculated for each overpass, and normalized to a sun angle of $\mu = 0.45$, using the theoretical relationships in Figs. 2-4, 2-5, and 2-6. The variation of $(C_o/C_R - 1)$ with sun angle is due to the variation of C_R alone. The function $(C_o/C_R - 1)$ is plotted in Fig. 4-6 against the aerosol content, as defined in Section 4.2.1, for MSS 4, 5 and 6. The intercept of the abscissa is determined for the hypothetical case of no atmosphere when $C_o = C_R$, and is given by the negative value of $(\tau_R/\tau_A)N$ where τ_R is the Rayleigh optical thickness, τ_A is the Elterman 1964 model aerosol optical thickness, both for the center wavelength of the particular MSS channel, and N is the Elterman 1964 model aerosol content.

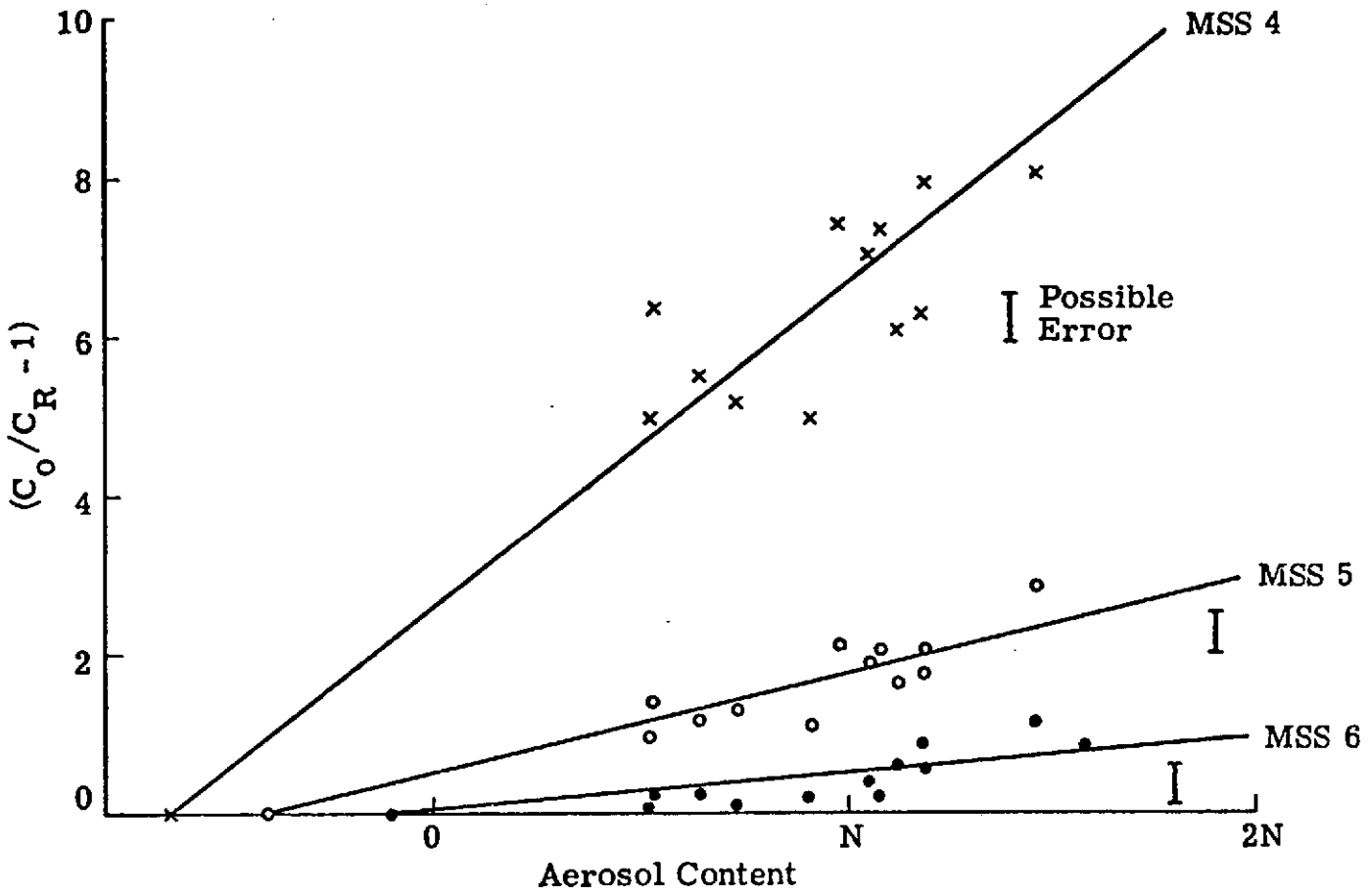

Fig. 4-6. $(C_o/C_R - 1)$ vs. Aerosol Content
(Normalized to sun angle $\mu = .45$)

Figure 4-6 shows that good linear relationships exist for MSS 4, 5 and 6; MSS 7 is not considered due to its low inaccurate radiance values over water. The results show that the contrast function becomes more sensitive to aerosol changes as the wavelength decreases. This is due to the increased atmospheric optical thickness at the shorter wavelengths. It should be noted that, since the radiance over the desert surface is not very sensitive to aerosol changes (see Section 4.2.2), the contrast function depends mainly on the radiance over the water surface.

When the instrument errors, discussed in Section 4.3, are considered, it is seen that MSS 6 is not sensitive enough, but that MSS 4 and 5 could be used for this technique and that they have comparable accuracy. If the mean straight lines are correct, then the instrument error in both MSS 4 and 5 would produce about $\pm$ 10% errors for the normal aerosol content. The scatter of data points about the mean line in Fig. 4-5 is due to measurement errors in the desert radiance, and due to errors in the assumptions concerning the contrast dependence on wavelength and sun angle, which can be examined only with independent measurements of these properties.

4.3 Error Analysis

The results of the analyses of the radiance-aerosol content and contrast-aerosol content relationships contain uncertainties due to inherent instrument errors, and due to the assumptions necessary in the data interpretation. These uncertainties are discussed below.

4.3.1 Volz Photometer Errors

Flowers et al, [19] in comparing the Volz photometer with a standard photometer, found that values of aerosol optical thickness greater than about .240 (i.e., an aerosol content of 1.13 N), can be measured with an

accuracy of ±5%, and for an optical thickness near .100 (.47 N), an accuracy of about ± 10% applies. It is presumed that similar errors apply to the measurements made in this program with our Volz photometer, and are indicated in Figs. 4-1 and 4-2.

A further error is possible in using the Volz data in this investigation due to the fact that the Volz measurement was never made directly over the water surface where the ERTS radiance measurement is made. It has been assumed that the atmosphere has been homogeneous over the area including the Volz and the radiance measurements. This may not always be a good assumption since the Volz data in Fig. 4-1, on occasion, show variations over a short time period, greater than the instrument error, suggesting the movement of air cells with different aerosol content. This type of error cannot be readily estimated, but could be checked in a future program, using several photometers in the test site area.

4.3.2 ERTS Radiance Errors

Fraser[26] has made calculations of the noise equivalent radiance for each of the MSS channels based on preflight calibrations. No inflight calibrations have been reported, and it is assumed that the preflight ones have not changed during this program. Fraser's results are reproduced in Table 4-4, with the values of the full scale radiance, and NER in radiance units added for clarity. If the radiance-aerosol content relationship in Fig. 4-2 is assumed to be correct, and the reduction in noise achieved by averaging over a 300m x 300m area (approximately 25 resolution elements) is taken into account, then the NER results in about a ± 10% error in determining the aerosol content in the useful channels MSS 4, 5 and 6.

If the radiance-aerosol content relationship in Fig. 4-2 is assumed to be correct, then the NER results in a ± 10% error in determining the

aerosol content in the useful channels MSS 4, 5 and 6. A similar uncertainty of ± 10% in the aerosol content also results from the NER in the contrast-aerosol content relationships for MSS 4 and 5 shown in Fig. 4-6.

With the limited set of data obtained during this program, certain assumptions were necessary regarding the reflectance of water and the desert as a function of wavelength and sun angle. These assumptions, as discussed in Section 4.2, were based on available measurements and theoretical models, and the uncertainties introduced cannot be readily estimated. The relatively small scatter of data in the linear relationships suggest that the assumptions are not unreasonable.

TABLE 4-4

The noise equivalent radiance (NER) for a single resolution element of MSS for ocean observations. Also the ratio of the standard deviation in sensor response to atmospheric turbidity changes to the NER. The mean sensor output (V), the standard deviation (σ), and NER are expressed in percentage of full scale sensor response (after Fraser[26]).

Spectral Band in μm	Surface Reflectivity	$\bar{V}$	σ	SNR	$\bar{V}$/SNR	σ/NER	Full Scale Radiance (mw/cm²/sr)	NER mw/cm²/ μm/sr
0.5-0.6 (MSS 4)	0.02	12	1.4	22	0.6	2.5	2.48	.15
	0.10	23	1.1	40	0.6	1.9		
0.6-0.7 (MSS 5)	0.02	8	1.4	9	0.9	1.5	2.00	.18
	0.10	22	1.0	22	1.0	1.0		
0.7-0.8 (MSS 6)	0.02	7	1.0	11	0.6	1.6	1.76	.11
	0.10	22	1.0	25	0.9	1.1		
0.8-1.1 (MSS 7)	0.02	4	0.5	3	1.0	0.5	4.60	.15
	0.10	10	0.4	10	0.9	0.4		

5. CONCLUSIONS

Significant results, relating the radiance over water surfaces to the atmospheric aerosol content, have been obtained. The results indicate that the MSS channels 4, 5 and 6 centered at 0.55, 0.65 and 0.75 μm have comparable sensitivity, and that the aerosol content can be determined within ± 10% with the assumed measurement errors of the MSS. The fourth channel, MSS 7, is not useful for aerosol determination due to the water radiance values for this channel generally being less than the instrument noise. The accuracy of the aerosol content measurement could be increased by using an instrument specifically designed for this purpose. In an independent study[27] we designed a simple instrument in which the radiance could be measured to ± 1% accuracy resulting in a ± 1.5% error in the aerosol content.

This radiance-aerosol content relationship can provide a basis for monitoring the atmospheric aerosol content on a global basis, allowing a base-line value of the global burden of aerosols to be established. This base-line could be established more rapidly from satellite measurements than from a network of ground-based observations, and probably with considerable cost savings. In addition, this technique could provide a method for monitoring the particulate emissions of the SST's, which are of concern to the Department of Transportation, by making observations in the vicinity of flight corridors, such as over the North Atlantic. It should be possible to look at the ocean through the flight corridor and alongside it, to measure the difference due to the SST's in the aerosol content.

Further studies of the radiance-aerosol content relationship should be made to establish the global applicability of the results, and to confirm that the effects of sun glitter are minimal as indicated in this program.

These studies could utilize future ERTS-1 and ERTS-B data at the existing test sites. Cooperation with other agencies such as EPA and NOAA, who make Volz observations, would allow the studies to be expanded to national and global scales. ERTS-1 data obtained over the USA since August 1972 could also be analyzed in conjunction with aerosol data from the turbidity network of Volz photometers operated by EPA.

The contrast-aerosol content investigation showed useful linear relationships in MSS channels 4 and 5, allowing the aerosol content to be determined within $\pm$ 10%. MSS 7 is not useful due to the low accuracy in the water radiance, and MSS 6 is found to be too insensitive. These results rely on several assumptions due to the lack of ground-truth data, but do serve to indicate which channels are most useful.

Future studies of this contrast relationship should use a different target where the radiances over both surfaces are affected significantly by aerosol changes. Possibly the Salton Sea/Imperial Valley area, or the San Diego bay/city area could be used, but several simultaneous Volz observations would be needed to assure homogeneity of the aerosol content over the target. The data from the EPA turbidity network should be examined for suitable target areas to investigate this relationship with existing ERTS data.

6. REFERENCES

1. "Study of Critical Environmental Problems (SCEP)," MIT Press (1970).

2. "Study of Man's Impact on Climate (SMIC)," MIT Press (1971).

3. M. T. Ellis and R. F. Pueschel, Science 172, 845 (1971).

4. G. M. Hidy and J. R. Brock, Second International Clean Air Congress, Washington, D. C. (Dec. 1970).

5. R. A. McCormick and J. H. Ludwig, Science 156, 1358 (1967).

6. G. D. Robinson, "Long-Term Effects of Air Pollution," Center for the Environment and Man, Inc., Hartford, Rept. No. CEM 4029-400 (1970).

7. R. J. Charlson and M. J. Pilat, J. Appl. Meteor. 8, 1001 (1969).

8. M. A. Atwater, Science 170, 64 (1970).

9. J. M. Mitchell, Jr., J. Appl. Meteor. 10, 703 (1971).

10. C. B. Ludwig, M. Griggs, W. Malkmus and E. R. Bartle, "Monitoring of Air Pollution by Satellites," NASA CR-112137, (April 1972).

11. M. Griggs, J. Air Poll. Contr. Assoc. 22, 356, (1972).

12. G. N. Plass and G. W. Kattawar, Appl. Opt. 7, 1129 (1968).

13. G. N. Plass and G. W. Kattawar, Appl. Opt. 9, 1122 (1970).

14. G. N. Plass and G. W. Kattawar, Appl. Opt. 11, 1598 (1972).

15. S. Q. Duntley, J. Opt. Soc. Am. 38, 179 (1948).

16. K. L. Coulson, G. M. Bouricius and E. L. Gray, G. Geophys. Res. 70, 4601 (1965).

17. K. L. Coulson, Appl. Opt. 5, 905 (1966).

18. J. I. Gordon and P. V. Church, Appl. Opt. 5, 919 (1966).

19. E. C. Flowers, R. A. McCormick and K. R. Kurfis, J. Appl. Meteor. 8, 955 (1969).

20. L. Elterman, AFCRL Rept. No. AFCRL-68-0153 (1968).

21. L. Elterman, in "Handbook of Geophysics and Space Environments," S. L. Valley, Ed. (McGraw-Hill Book Co., New York, 1965).

22. R. Fraser, Private Communication. Dr. Fraser determined the radiance, and the Volz measurement was made from a NOAA ship.

23. M. Griggs, J. Appl. Meteor. 7, 1012 (1968).

24. E. V. Ashburn and R. G. Weldon, J. Opt. Soc. Am. 46, 583 (1956).

25. M. Griggs and W. Marggraf, "Measurement of Cloud Reflectance Properties and the Atmospheric Attenuation of Solar and Infrared Energy," Final Rept. General Dynamics Convair, San Diego, AFCRL-68-0003 (1967).

26. R. Fraser, Private Communication.

27. "Monitoring of Air Pollution by Satellites (MAPS)," Phase I Rept., Contract NAS1-12048, Science Applications Rept. SAI-73-564-LJ, (June 1973).